DOI: 10.1002/zaac.200500430

Characterization of Mixed Crystals in the System $Cu_2Mn_xCo_{1-x}GeS_4$ and Investigations of the Tetrahedra Volumes

Thomas Bernert and Arno Pfitzner

Regensburg, Institut für Anorganische Chemie der Universität

Received November 3rd, 2005.

Professor Hanskarl Müller-Buschbaum zum 75. Geburtstag gewidmet

Abstract. In a series of investigations on normal tetrahedral compounds we present mixed crystals in the system $Cu_2Mn_xCo_{1-x}GeS_4$ ($0 < x < 1$) and an inspection of their tetrahedra volumes. Cu_2CoGeS_4 crystallizes tetragonal in a stannite type structure, Cu_2MnGeS_4 crystallizes orthorhombic in the wurtzstannite structure type. The crystal structures of Cu_2CoGeS_4 and $Cu_2Mn_{0.68}Co_{0.32}GeS_4$ were refined from single crystal diffraction data. The refinement of Cu_2CoGeS_4 converged to $R = 0.0547$ and $wR2 = 0.0847$ for 299 unique reflections. The refinement of $Cu_2Mn_{0.68}Co_{0.32}GeS_4$ converged to $R = 0.0481$ and $wR2 = 0.0877$ for 1556 unique reflections. From these data the tetrahedra volumes of the end members and of $Cu_2Mn_{0.68}Co_{0.32}GeS_4$ are calculated. In Cu_2CoGeS_4 tetrahedra $[MS_4]$ are similar in size. In contrast, the differences of the volumes of the polyhedra $[MS_4]$ in the orthorhombic wurtzite superstructure type compounds Cu_2MnGeS_4 and $Cu_2Mn_{0.68}Co_{0.32}GeS_4$ are significant (M = Cu, Mn, ($Mn_{0.68}Co_{0.32}$), Co, Ge). From $x = 0$ to $x = 0.5$ the tetragonal structure type dominates while from $x = 0.7$ to the Cu_2MnGeS_4 end member the products crystallize in the orthorhombic structure type. Melting points of the mixed crystals decrease linearly with increasing manganese content.

Keywords: Wurtzite superstructure type; sphalerite superstructure type; solid solution series; quaternary compounds

Introduction

One can derive binary and multinary compositions from an element of group 14 by using the so-called cross-substitution method. The derived tetrahedral compounds are of interest because of their magnetical, optical or semiconducting properties, e.g. [1−5]. Tetrahedral compounds are classified as normal- or defect tetrahedral compounds. Adamantane structures are one group of tetrahedral compounds. Therein each cation is coordinated by four anions and vice versa. The prediction which compositions can form tetrahedral or adamantane structures is described in detail by *E. Parthé*, see [6] for a survey.

Quaternary compounds of the general composition $M^{I}_2M^{II}M^{IV}Q_4$ are in the focus of research since a long time. First investigations were performed in the 1960ies. *Hahn* and *Schulze* started X-ray powder diffraction investigations on germanium and tin containing materials [7]. *Schäfer* and *Nitsche* were the first authors to report on Si containing compounds [8, 9]. They synthesized and investigated more than 30 compounds of the above mentioned type by X-ray powder diffraction, including M^{II} = Mn, Fe, Co, Ni, Zn, Cd, Hg and M^{IV} = Si, Ge, Sn. Further publications added tellurides, e.g. [1, 10, 11], and quaternary silver chalcogenides, e.g. [12−16], to the known compounds. Even materials with lead as the M^{IV}-ion were reported [17]. X-ray powder diffraction investigations on $M^{I}_2Mn M^{IV}Q_4$ compounds (M^{I} = Cu, Ag, M^{IV} = Si, Ge, Sn, Q = S, Se, Te) were introduced by *Lamarche* et al. [18]. Mixed crystals in the system $Cu_2Zn_{1-x}Mn_xGeS_4$ were described by *Honig* and co-workers [19]. In the last years there was a strong interest in quasi ternary phase diagrams of the type $M^{I}_2Q - M^{II}Q - M^{IV}Q_2$. In the course of these investigations crystal structures of many quaternary tetrahedral compounds were refined by Rietveld methods [20].

Attempts to predict the structure type of normal tetrahedral materials were made for binary and ternary compounds [21, 22]. Our new approach concerning the structure prediction of ternary and multinary tetrahedral materials was first presented in [23]. An inspection of the crystal structures of Cu_3SbS_4 and Cu_3PS_4 revealed that tetrahedra $[MS_4]$ (M = Cu, P, Sb) in the sphalerite superstructure type compound Cu_3SbS_4 are quite similar in size while they differ significantly in the wurtzite superstructure type (wurtzstannite type) Cu_3PS_4. We are of the opinion that the hexagonal anion packing tolerates distortions caused by the differences in the size of the tetrahedra $[MQ_4]$ better than the cubic anion arrangement. In these terms we discussed mixed crystals in the system $Cu_3As_xSb_{1-x}S_4$ and introduced a mathematical concept for a quantitative consideration of

* Prof. Dr. Arno Pfitzner
Institut für Anorganische Chemie
Universität Regensburg
Universitätsstr. 31
D-93040 Regensburg
Fax: +49(0)941 / 943-4983
E-mail: arno.pfitzner@chemie.uni-regensburg.de

the tetrahedra volumes. We also included compounds from the literature in our calculations [24]. In further work we concentrated on quaternary compounds of the type $Cu_2Mn\mathit{M}^{IV}S_4$ (M^{IV} = Si, Ge, Sn) [25]. Elementary for this work was an observation by Schäfer et al. They pointed out that in many quaternary compounds of the just mentioned type including Co, Hg, Zn, Cd, Ni as the M^{II}-ion, compounds with Si as the M^{IV}-ion are always found to crystallize in the wurtzite type while tin compounds form cubic anion arrangements. Compounds with M^{IV} = Ge cannot be associated preferentially to one of both structure types [9]. Therefore we investigated mixed crystals in the system Cu_2MnGeS_4 (wurtzstannite) − Cu_2MnSnS_4 (stannite) for a better understanding of the influence of the M^{IV}-cation on the structure type [26]. It seems to be desirable to check also the influence of the M^{II}-cation. With Cu_2CoGeS_4 a germanium containing compound is found to crystallize as a sphalerite variant. Herein we report on our investigations of materials of the composition $Cu_2\mathit{M}^{II}GeS_4$, i.e. on the influence of variation on the position of the divalent cation. We present mixed crystals in the system $Cu_2Mn_xCo_{1-x}GeS_4$ ($0 < x < 1$) and compare the tetrahedra volumes with those described in [25] and [26].

The crystal structure of Cu_2CoGeS_4 was already refined by *Gulay* et al. from X-ray powder diffraction data [27]. As the consideration of the tetrahedra volumes requires a very precise evaluation of the bond lengths a redetermination of the structure from single crystal data is performed.

It should be mentioned that a similar concept to separate tetrahedral structures based on the distortions of the different tetrahedra [MQ_4] was published by *Parasyuk* et al. in 2005 [20]. Their argumentation bases on the ionic radii of the metal ions in quaternary tetrahedral compounds. We expect our concept to be more applicable as it is based on experimental structural data instead of empirical averaged data. Averaging data can lead to erroneous conclusions as it becomes evident from our latest results [26]. However, both concepts are tools to reconsider the quality and correctness of older structure refinements.

Experimental

Cu_2MnGeS_4 and Cu_2CoGeS_4 were prepared from stoichiometric mixtures of the elements in evacuated fused silica ampoules. The ampoules were coated with pyrolytic carbon prior to use in order to avoid reaction with the educts (metals: AlfaAesar 99.999 %, sulphur: Riedel de Haën 99.999 %). After two heating periods of three days (900 °C in the case of Cu_2CoGeS_4 and 800 °C for Cu_2MnGeS_4) with intervening homogenisation pure products were obtained as shown by X-ray powder diffraction. These products were utilized as starting materials to prepare the solid solution series. Mixed crystals were annealed at 800 to 850 °C for 5 days, homogenized in an agate ball mill and then pressed to pellets. These were annealed again for 5 days at the same temperature. The purity of the mixed crystals was also checked by X-ray powder diffraction on a STOE Stadi P ($CuK\alpha_1$, germanium monochromator). Thermal analyses were carried out on a Setaram TMA 90 16.18 high temperature DTA. All samples were heated to 1200 °C and cooled down to room temperature with a rate of 10 K per minute. Single crystals of Cu_2CoGeS_4 and $Cu_2Mn_{0.68}Co_{0.32}GeS_4$ suitable for structure analysis were selected under a microscope and fixed on glass capillaries. Single crystal X-ray diffraction data were collected on an Oxford Xcalibur S and a STOE IPDS II, respectively. The composition of the mixed crystal was refined to $x = 0.680$ (4). A statistical distribution of Mn and Co on the 2*a* site is found. Table 1 lists all details of the measurements and refinements.

Tables 2 and 3 provide atomic parameters, isotropic, and anisotropic displacement parameters for Cu_2CoGeS_4. In Tables 4 and 5 these values are collected for $Cu_2Mn_{0.68}Co_{0.32}GeS_4$.

Results and Discussion

Lattice constants and c/a-ratios

X-ray powder diffraction diagrams taken from samples which were rapidly cooled from the annealing temperature in air indicate a miscibility gap in the system $Cu_2Mn_xCo_{1-x}GeS_4$. The stannite structure type reaches from the pure Co containing end member to $x = 0.5$. In the powder pattern of this sample the orthorhombic phase could already be observed although these reflections were small in intensity. The diffraction pattern of the sample with $x = 0.6$ clearly showed reflections of both phases, the tetragonal and the orthorhombic one. Here, both phases could be indexed. Samples with $x = 0.7$ to $x = 1.0$ contained only the orthorhombic modification. The cell volumes increase linearly with increasing Mn content, see Figure 1. Mn^{2+} is larger than Co^{2+} by 0.08 Å concerning ionic radii derived from [32]. For "$Cu_2Mn_{0.6}Co_{0.4}GeS_4$" the volumes of both phases are plotted in Figure 1. The point that hits the line corresponds to the volume of the orthorhombic phase. The cell volume of the tetragonal material is smaller. The evolution of the lattice constants *a* and *c* of the tetragonal samples with the composition is shown in Figures 2 and 3. Both lattice constants increase with increasing Mn content similar to the cell volumes.

We calculated the *c*/*a*-ratios for the tetragonal reaction products. The ideal stannite structure type has a *c*/*a*-ratio of 2.0. The cubic unit cell of sphalerite is doubled in *c* direction by ordering of the cations, thus leading to the tetragonal superstructure. The *c*/*a*-ratios increase linearly with increasing content of Mn as demonstrated in Figure 4. This means the composition $Cu_2Mn_{0.4}Co_{0.6}GeS_4$, $c/a = 1.9863$, has the closest value to $c/a = 2$. Reflections in the powder diagram show a splitting that becomes more evident with increasing deviations of the ideal value. As the pure end member Cu_2CoGeS_4 shows the strongest deviation with $c/a = 1.9776$ the splitting of the lines decreases with increasing Mn content.

Thermal analysis

The melting behaviour of the mixed crystals was investigated by thermal analyses. All samples were heated twice to 1200 °C in order to detect incongruent melting or decomposition. In all cases the peaks indicating the melting

Table 1 Crystallographic data for the X-ray structure determinations of Cu_2CoGeS_4 and $Cu_2Mn_{0.68}Co_{0.32}GeS_4$.[a)]

Compound	**Cu_2CoGeS_4**	**$Cu_2Mn_{0.68}Co_{0.32}GeS_4$**
Formula weight / g mol^{-1}	386.84	385.24
Crystal size / mm^3	0.15 × 0.18 × 0.20	0.25 × 0.10 × 0.12
Crystal colour	black	black
Crystal system	tetragonal	orthorhombic
Spacegroup	$I\bar{4}2m$ (No. 121)	$Pmn2_1$ (No. 31)
Lattice constants / Å	a = 5.307 (2)	a = 7.577 (2)
from single crystal	c = 10.493 (5)	b = 6.509 (1)
measurements		c = 6.233 (1)
Cell volume / Å^3, Z	295.5 (2), 2	307.4 (1), 2
$\rho_{X\text{-ray}}$ / g cm^{-3}	4.348	4.162
Diffractometer	Oxford Xcalibur S, Mo$K\alpha$, λ = 0.71073 Å, graphite monochromator	STOE IPDS II, Mo$K\alpha$, λ = 0.71073 Å, graphite monochromator
Detector distance / mm	50.0	100.0
Absorption coefficient/ mm^{-1}	16.162	15.276
Absorption correction	numerical, CrysAlis RED [28]	numerical, crystal shape optimized with X-SHAPE [29]
Temperature / °C		20
θ-range / °	3.88 < θ < 32.68	4.13 < θ < 36.54
hkl-range	$-5 \le h \le 7$	$-11 \le h \le 12$
	$-8 \le k \le 7$	$-8 \le k \le 10$
	$-15 \le l \le 15$	$-10 \le l \le 10$
No. of reflections, $R_{int.}$, R_σ	2237, 0.0690, 0.0377	5827, 0.0597, 0.0411
No. of independent reflections	299	1556
No. of parameters	15	45
Extinction coefficient	0.057 (5)	0.0894 (7)
Weighting parameters a and b[b)]	0.0173, 2.5979	0.0448, 0
Completeness of data	99.5 %	99.1 %
Flack parameter	−0.04 (5)	0.00 (1)
Program	SHELX97 [30, 31]	
R ($I > 2\sigma_I$), R (all reflections)[b)]	0.0326, 0.0547	0.0383, 0.0481
$wR2$ ($I > 2\sigma_I$), $wR2$ (all reflections)[b)]	0.0788, 0.0832	0.0841, 0.0877
GooF[b)]	1.178	1.065
Largest difference peaks $\Delta\rho_{max}$, $\Delta\rho_{min}$ in e Å^{-3}	0.587, −0.825	1.620, −1.379

[a)] Further details of the crystal structure investigations are available from the Fachinformationszentrum Karlsruhe, Gesellschaft für wissenschaftlich-technische Information mbH, D-76344 Eggenstein-Leopoldshafen (Germany) on quoting the depository numbers CSD 415927 (Cu_2CoGeS_4), and CSD 415926 ($Cu_2Mn_{0.68}Co_{0.32}GeS_4$), the name of the authors, and citation of the publication.

[b)] $R = \frac{\Sigma||F_o|-|F_c||}{\Sigma|F_o|}$, $wR_2 = \sqrt{\frac{\Sigma[w(F_o^2 - F_c^2)^2)]}{\Sigma[w(F_o^2)^2]}}$, $GooF = S = \sqrt{\frac{\Sigma[w(F_o^2 - F_c^2)^2]}{n-p}}$ (n = no. of reflections, p = no. of parameters), $w = \frac{1}{(\sigma^2(F_o^2) + (aF_o)^2 + bP)}$, $P = [2F_c^2 + Max(F_o^2, 0)]/3$

Table 2 Atomic coordinates (e.s.d.s) and U_{eq}[a] (in Å^2) for Cu_2CoGeS_4.

Atom	Wyckoff position	x	y	z	U_{eq}
Cu	*4d*	$^1/_2$	0	$^3/_4$	0.0131 (5)
Co	*2b*	$^1/_2$	$^1/_2$	$^1/_2$	0.0193 (7)
Ge	*2a*	0	0	$^1/_2$	0.0192 (7)
S	*8i*	0.2442 (4)	x	0.6275 (2)	0.0118 (4)

[a)] U_{eq} is defined as one third of the trace of the orthogonalized U_{ij} tensor.

Table 3 Anisotropic displacement parameters U_{ij} (in Å^2) for Cu_2CoGeS_4.

Atom	$U_{11} = U_{22}$	U_{33}	U_{12}	$U_{13} = U_{23}$
Cu	0.0123 (5)	0.0148 (8)	0	0
Co	0.021 (1)	0.017 (1)	0	0
Ge	0.0202 (8)	0.017 (1)	0	0
S	0.0120 (5)	0.0115 (8)	−0.0022 (8)	0.0000 (6)

Table 4 Atom coordinates (e.s.d.s) and U_{eq}[a] (in Å^2) for $Cu_2Mn_{0.68}Co_{0.32}GeS_4$.

Atom	Wykoff position	x	y	z	U_{eq}
Cu	4*b*	0.24843 (1)	0.32440 (2)	0.71371 (1)	0.02026 (3)
Ge	2*a*	0	0.82635 (2)	0.70616 (1)	0.01020 (2)
M*	2*a*	0	0.15845 (3)	0.20402 (3)	0.01552 (4)
S1	2*a*	0	0.15017 (4)	0.59278 (4)	0.01245 (5)
S2	2*a*	0	0.81582 (4)	0.06447 (4)	0.01241 (6)
S3	4*b*	0.23713 (2)	0.66174 (3)	0.58329 (3)	0.01230 (4)

[a] see footnote for table 2.
* *M* represents the site statistically occupied by Mn and Co.

process did not change in the second heating cycle. So no evidence for decomposition of the samples was found. The melting points decrease linearly with increasing Mn content. Figure 5 depicts the evolution of the melting points (onset points) with the composition. *Schäfer* and *Nitsche* already determined the melting points of Cu_2CoGeS_4 and

Table 5 Anisotropic displacement parameters U_{ij} (in Å^2) for $Cu_2Mn_{0.68}Co_{0.32}GeS_4$.

Atom	U_{11}	U_{22}	U_{33}	U_{12}	U_{13}	U_{23}
Cu	0.02170 (5)	0.02121 (5)	0.01788 (6)	0.00142 (4)	0.00101 (4)	−0.00108 (5)
Ge	0.01152 (4)	0.01003 (4)	0.00907 (4)	0	0	−0.00041 (5)
*M**	0.01541 (7)	0.01692 (7)	0.01422 (6)	0	0	0.00017 (8)
S1	0.0147 (1)	0.00932 (9)	0.0134 (1)	0	0	0.00116 (9)
S2	0.0137 (1)	0.0160 (1)	0.00757 (8)	0	0	0.00034 (9)
S3	0.01340 (7)	0.01293 (8)	0.01055 (7)	0.00198 (6)	0.00186 (6)	−0.00008 (7)

* *M* represents the site statistically occupied by Mn and Co.

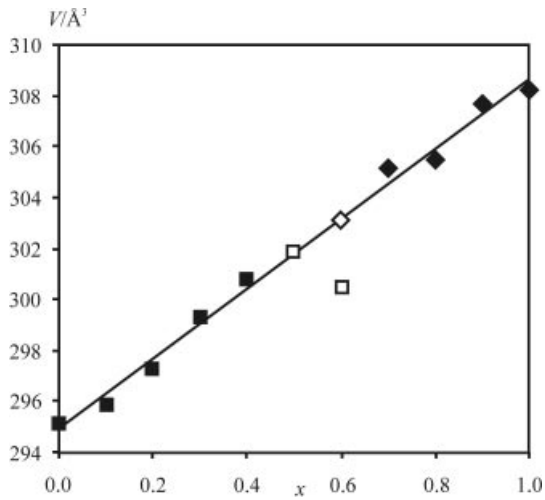

Figure 1 Unit cell volumes in the system $Cu_2Mn_xCo_{1-x}GeS_4$ vs. the composition x. The same symbols are used for all Figures. Filled: pure samples, open: two phase samples. ■ tetragonal compounds, ◆ orthorhombic materials.

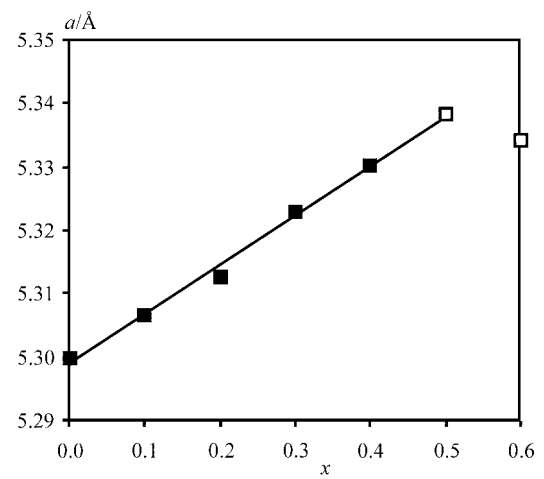

Figure 2 Lattice parameter a vs. the composition x for the tetragonal products. Open symbols represent two phase samples. The point at $x = 0.6$ was not used for linear regression.

Cu_2MnGeS_4 to 1031 °C and 994 °C, respectively. Both compounds are reported to melt congruently [9].

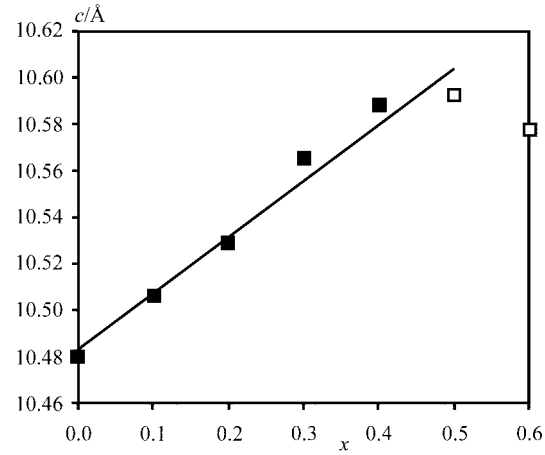

Figure 3 Lattice parameter c vs. the composition x for the tetragonal products. Open symbols represent two phase samples. The point at $x = 0.6$ was not used for linear regression.

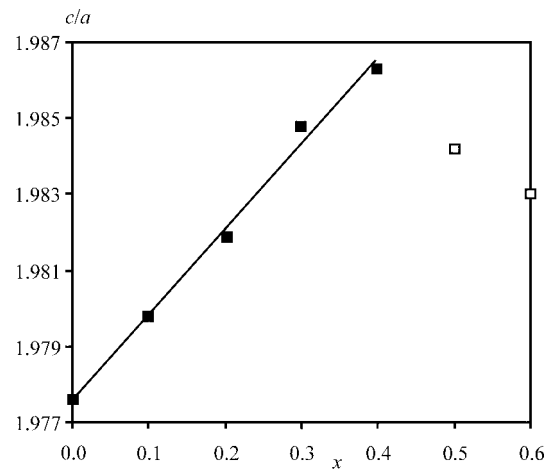

Figure 4 Ratios c/a of the tetragonal samples vs. the composition x for the tetragonal products. Open symbols represent two phase samples. These two points were not used for linear regression.

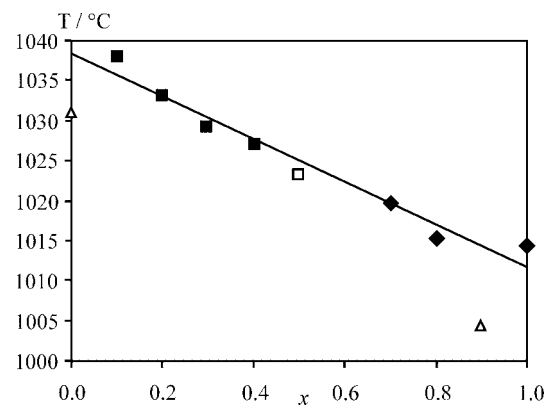

Figure 5 Melting points in the system $Cu_2Mn_xCo_{1-x}GeS_4$. Points marked by triangles are not used for linear regression.

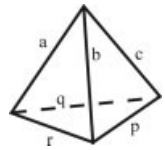

Figure 6 Labelling of the tetrahedra edges [33]

Tetrahedra volumes

In order to obtain one significant value for a compound that describes the differences in size of the different tetrahedra [MQ_4], the so-called $\overline{\Delta V_i}$-value was defined in [24]. First the volumes of the tetrahedra have to be calculated. This is done using the following formula (labelling of the tetrahedra edges follows Figure 6):

$$V = \left(\frac{1}{288} \cdot \begin{vmatrix} 0 & r^2 & q^2 & a^2 & 1 \\ r^2 & 0 & p^2 & b^2 & 1 \\ q^2 & p^2 & 0 & c^2 & 1 \\ a^2 & b^2 & c^2 & 0 & 1 \\ 1 & 1 & 1 & 1 & 0 \end{vmatrix} \right)^{\frac{1}{2}} \quad [33] \tag{1}$$

From the volumes of all tetrahedra the average volume is calculated:

$$\overline{V} = \frac{\sum_1^n V_i}{n} \tag{2}$$

$$\Delta V_i = \frac{V_i - \overline{V}}{\overline{V}} \tag{3}$$

The stoichiometry of the samples has to be taken into account. The differences for each tetrahedron to the mean value are computed in per cent:

Finally all differences ΔV_i are averaged to the $\overline{\Delta V_i}$-value.

$$\overline{\Delta V_i} = \frac{\sum_i |\Delta V_i|}{i} \tag{4}$$

Table 6 ΔV_i- and $\overline{\Delta V_i}$-values of $Cu_2Mn_{0.68}Co_{0.32}GeS_4$ and the end members.

Compound	ΔV_i [CuS_4]/%	ΔV_i [GeS_4]/%	ΔV_i [$M^{IV}S_4$]/%	$\overline{\Delta V_i}$
Cu_2MnGeS_4	−1.3	−12.9	15.4	7.7
$Cu_2Mn_{0.68}Co_{0.32}GeS_4$	−0.6	−11.9	13.0	6.4
Cu_2CoGeS_4	−1.9	−2.8	6.7	3.3

Table 6 contains ΔV_i- and $\overline{\Delta V_i}$-values for Cu_2CoGeS_4, $Cu_2Mn_{0.68}Co_{0.32}GeS_4$, and Cu_2MnGeS_4. The value for Cu_2MnGeS_4 already has been reported in [25] and in [26].

The two materials of the wurtzstannite type, Cu_2MnGeS_4 and $Cu_2Mn_{0.68}Co_{0.32}GeS_4$, have significantly larger $\overline{\Delta V_i}$-values than the stannite type compound Cu_2CoGeS_4. The evolution of the ΔV_i-values of the [$M^{IV}S_4$] polyhedra with the composition is shown in Figure 7. The values lie on a straight line. Figure 8 shows a comparison of the three structures emphasizing the different tetrahedra. Obviously, the polyhedra in Cu_2CoGeS_4 have about the same size while

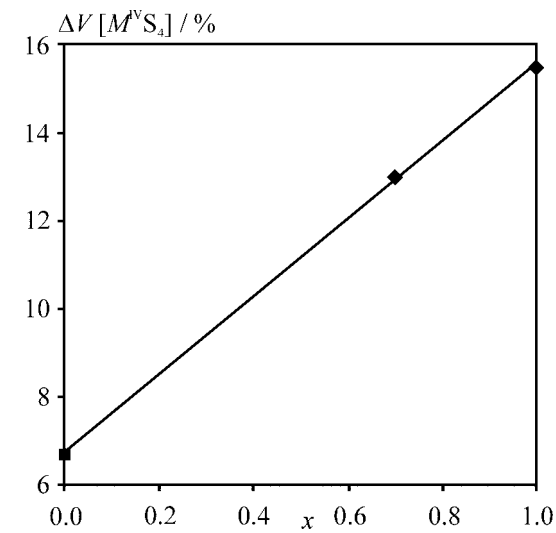

Figure 7 ΔV_i of the tetrahedra [MS_4] vs. the composition x.

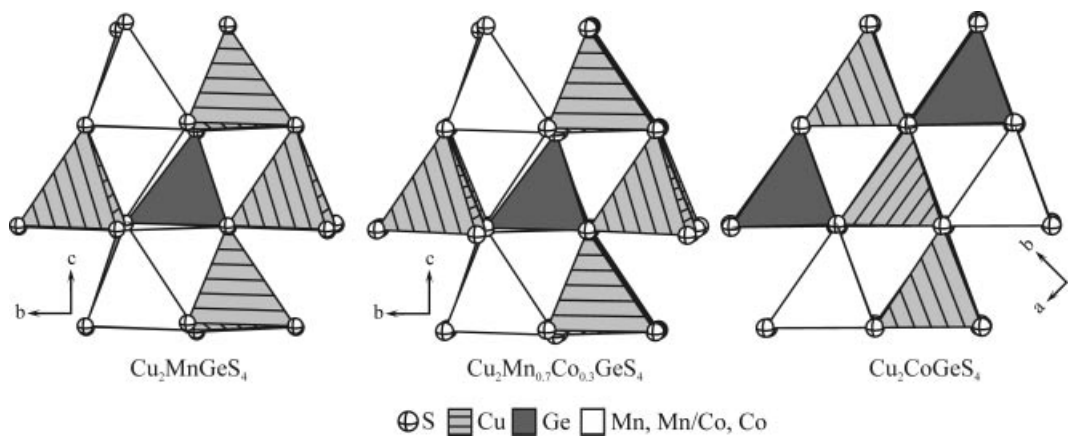

Figure 8 Sections of the crystal structures of Cu_2MnGeS_4, $Cu_2Mn_{0.68}Co_{0.32}GeS_4$, and Cu_2CoGeS_4. The differences in size of the tetrahedra [MS_4] are most significant in the manganese end member and are also remarkable in $Cu_2Mn_{0.68}Co_{0.32}GeS_4$. Contrary, the tetrahedra have about the same size in the stannite type compound Cu_2CoGeS_4.

tetrahedra in the two wurtzstannite type compounds differ significantly. The differences between the wurtzstannite variants are not apparent.

As already reported in [24] there is no sharp border line between the $\overline{\Delta V_i}$-values of the two structure types with different packing of the anions. Instead, an overlap area can be found between $\overline{\Delta V_i} = 5$ and $\overline{\Delta V_i} = 8.5\,\%$. Compounds that crystallize in both modifications fall in this two phase region, e.g. Cu_3AsS_4 (luzonite and enargite).

The $\overline{\Delta V_i}$-value for Cu_2CoGeS_4 clearly is in the range for sphalerite type structures, that is $\overline{\Delta V_i} < 5\,\%$. The values for the other two compounds are in the overlap area but closer to the higher values, i.e. for wurtzite type compounds. As accounted in [26] there exists also a tetragonal modification of Cu_2MnGeS_4. Comparing these values for the compounds under discussion with the ones in [26] one can see that Cu_2CoGeS_4 can be clearly related to the stannite type. $\overline{\Delta V_i}$ of Cu_2MnSnS_4 (stannite type) is 6.1. It is slightly smaller than the value for $Cu_2Mn_{0.68}Co_{0.32}GeS_4$ ($\overline{\Delta V_i} = 6.4$, wurtzstannite type). Finally the value for Cu_2MnSiS_4 ($\overline{\Delta V_i} = 11.1\,\%$) again clearly indicates the wurtzite superstructure type. Compounds with values within the overlap region either are mixed crystals with a composition between the pure wurtzstannite type and the pure stannite type end members or crystallize in both modifications like Cu_2MnGeS_4.

Acknowledgement. The authors thank *Dr. Hoffmann*, TU München, for collecting single crystal X-ray data.

References

[1] T. Hirai, K. Kurata, Y. Takeda, *Solid State Electron.* **1967**, *10*, 975.
[2] D. M. Schleich, A. Wold, *Mater. Res. Bull.* **1977**, *12*, 111.
[3] L. Guen, W. S. Glausinger, *J. Solid State Chem.* **1980**, *35*, 10.
[4] T. Fries, Y. Shapira, F. Palacio, M. C. Morón, G. J. McIntyre, R. Kershaw, A. Wold, E. J. McNiff, Jr, *Physical Review* **2004**, *B56*, 5424.
[5] H. Matsushita, T. Ichikawa, A. Katsui, *J. Mater. Sci.* **2005**, *40*, 2003.
[6] E. Parthé: Wurtzite and Sphalerite structures. In: *Crystal structures of Intermetallic Compounds.* (Eds. J. H. Westbrook, R. L. Fleischer) J. Wiley and Sons, New York, 2000.
[7] H. Hahn, H. Schulze, *Naturwissenschaften* **1965**, *52*, 426.
[8] W. Schäfer, R. Nitsche, *Mater. Res. Bull.* **1974**, *9*, 945.
[9] W. Schäfer, R. Nitsche, *Z. Kristallogr.* **1977**, *145*, 356.
[10] A. Dragunas, K. Makariunas, M. Balciuniene, *Phys. Status Solidi* **1983**, *A77*, 463.
[11] H. Haeuseler, F. W. Ohrendorf und M. Himmrich, *Z. Naturforsch.* **1991**, *46b*, 1049.
[12] R. Caye, Y. Laurent, P. Picot, R. Pierrot, C. Levy, *Bull. Soc. Fr. Mineral. Cristallogr.* **1968**, *91*, 383.
[13] E. Parthé, K. Yvon, R. H. Deitch, *Acta Crystallogr.* **1969**, *B25*, 1164.
[14] Z. Johan, P. Picot, *Bull. Mineral.* **1982**, *105*, 229.
[15] H. Haeuseler, M. Himmrich, *Z. Naturforsch.* **1989**, *44b*, 1035.
[16] J. C. Wooley, A.-M. Lamarche, G. Lamarche, C. Church, I. P. Swainson, T. M. Holden, *J. Solid State Chem.* **1995**, *115*, 192.
[17] M. Quintero, A. Barreto, P. Grima, R. Tovar, E. Quintero, G. Sánchez Porras, J. Ruiz, J. C. Woolley, G. Lamarche, A-M. Lamarche, *Mater. Res. Bull.* **1999**, *34*, 2263.
[18] A.-M. Lamarche, A. Willsher, L. Chen, G. Lamarche, J. C. Wooley, *J. Solid State Chem.* **1991**, *94*, 313.
[19] E. Honig, H-S. Shen, G-Q. Yao, K. Doverspike, R. Kershaw, K. Dwight, A. Wold, *Mater. Res. Bull.* **1988**, *23*, 307.
[20] O. V. Parasyuk, L. V. Piskach, Y. E. Romanyuk, I. D. Olekseyuk, V. I. Zaremba, V. I. Pekhnyo, *J Alloys Compds.* **2005**, *397*, 85, and references therein.
[21] M. E. Fleet, *Mater. Res. Bull.* **1976**, *11*, 1179.
[22] M. O'Keeffe, B. G. Hyde, *Acta Crystallogr.* **1978**, *B34*, 3519.
[23] A. Pfitzner, S. Reiser, *Z. Kristallogr.* **2002**, *217*, 51.
[24] A. Pfitzner, T. Bernert, *Z. Kristallogr*. **2004**, *219*, 20.
[25] T. Bernert, A. Pfitzner, *Z. Kristallogr.* **2005**, *220*, 968; T. Bernert, A. Pfitzner, *Z. Anorg. Allg. Chem.* **2004**, *630*, 1711.
[26] T. Bernert, A. Pfitzner, *J. Solid State Chem.* **2006**, *179*, 849.
[27] L. D. Gulay, O. P. Nazarchuk, I. D. Olekseyuk, *J. Alloys Compds.* **2004**, *377*, 306.
[28] CrysAlis RED, Oxford Diffraction Ltd., version 1.171.27p5 beta, Abingdon, Oxfordshire, England, 2005
[29] STOE & Cie GmbH Darmstadt, 1996, 1997, Crystal optimisation for numerical absorption correction.
[30] G. M. Sheldrick: SHELXS97 Program for the solution of crystal structures, Universität Göttingen, 1997.
[31] G. M. Sheldrick: SHELXL97 Program for the refinement of crystal structures, Universität Göttingen, 1997.
[32] R. D. Shannon, *Acta Crystallogr.* **1976**, *A32*, 751.
[33] I. N. Bronstein, K. A. Semendjaev, *Taschenbuch der Mathematik*, Verlag Harry Deutsch, Zürich 1969.

